Protected Horticulture and Plant Factory, Vol. 29, No. 1:9-19, January (2020)
DOI https://doi.org/10.12791/KSBEC.2020.29.1.9
pISSN 2288-0992
eISSN 2288-100X

Measurement of Convective Heat Transfer Coefficients of Horizontal Thermal Screens under Natural Conditions

Adeel Rafiq[1], Wook Ho Na[2], Adnan Rasheed[1], Hyeon Tae Kim[3], and Hyun Woo Lee[1,2,4]*

[1]*Department of Agricultural Engineering, Kyungpook National University, Daegu 41566, Korea*
[2]*Institute of Agricultural Science and Technology, Kyungpook National University, Daegu 41566, Korea*
[3]*Department of Bio-Industrial Machinery Eng., Gyeongsang National Univ. (Insti. of Agric. & Life Sci.), Jinju 52828, Korea*
[4]*Smart Agriculture Innovation Center, Kyungpook National University, Daegu 41566, Korea*

Abstract. Convective heat transfer is the main component of greenhouse energy loss because the energy loss by this mechanism is greater than those of the other two components (radiative and conductive). Previous studies have examined the convective heat transfer coefficients under natural conditions, but they are not applicable to symmetric thermal screens with zero porosity, and such screens are largely produced and used in Korea. However, the properties of these materials have not been reported in the literature, which causes selectivity issues for users. Therefore, in this study, three screens having similar color and zero porosity were selected, and a mathematical procedure based on radiation balance equations was developed to determine their convective heat transfer coefficients. To conduct the experiment, a hollow wooden structure was built and the thermal screen was tacked over this frame; the theoretical model was applied underneath and over the screen. Input parameters included three components: 1) solar and thermal fluxes; 2) temperature of the screen, black cloth, and ambient air; and 3) wind velocity. The convective heat transfer coefficients were determined as functions of the air−screen temperature difference under open-air environmental conditions. It was observed from the outcomes that the heat transfer coefficients decreased with the increase of the air−screen temperature difference provided that the wind velocity was nearly zero.

Additional key words : absorption, convective heat transfer coefficient, pyranometer, thermal screens

Introduction

Convective heat loss represents one of the three basic modes of heat transfer, and it dominates over radiative and conductive heat loss (Papadakis et al., 1992; Kreith et al., 2012; Kakac et al., 2013). This thermal exchange phenomenon involves mass transfer (Baïri et al., 2014). Natural convection from horizontal, isothermal, and rectangular plates has been the subject of many experimental and theoretical investigations (Sharma and Adelman, 1969; Yang et al., 1991; Radziemska and Lewandowski, 2005; Corcione, 2008).

During this period, a large number of correlations have been developed to fit the heat transfer data (Khalifa, 2001). However, natural convection from horizontal screens has got lower consideration as compared to pure free convection from horizontal mechanical surfaces. The outcome is that information about horizontal screens is sometimes unpredictable, and the physical nature of the boundary layer flow is insufficiently known. Free convection from thermal screens is vital to the researchers and greenhouse growers.

The phenomenon of free, forced, and mixed convective heat transfer from greenhouse-covering materials and plastic shading nets to the natural environment has been previously investigated by few studies (Papadakis et al., 1992; Abdel-Ghany et al., 2015). These studies dealt with homogenous (screens made of one material only) and symmetric (screens with identical sides) materials. With the development of new greenhouse screens (heterogeneous and asymmetric), their application to new cases is limited.

In order to determine the convective heat transfer coefficient, it is necessary to know whether the exchange is due to free or forced convection or a combination of both (Papadakis et al., 1992). In convective heat transfer, two dimensionless numbers, the Reynolds number (Re) and Grashof number (Gr), are important for the characterization of flow. The ratio $Gr.Re^{-2}$ defines the importance of natural convection

*Corresponding author: whlee@knu.ac.kr
Received October 08, 2019; Revised November 28, 2019; Accepted December 03, 2019

with respect to forced convection (Issa and Lang, 2013).

It is well established that forced convection prevails when $Gr \cdot Re^{-2}$ 1, forced convection is negligible when $Gr \cdot Re^{-2}$ 1, and both natural and forced convection are significant when $Gr \cdot Re^{-2}$ 1 (Incropera et al., 2007).

In this study we describe a new radiation balance method for heterogeneous (made of more than one material) symmetric screens. The first purpose of this study is to determine the heat flux and convective heat transfer coefficient of greenhouse screens. The second is to draw a relationship between convective heat transfer coefficients, air velocity, and air–screen temperature differences. The final purpose is to separate natural, forced, and mixed convection by using the $Gr \cdot Re^{-2}$ ratio.

Materials and Methods

1. Material Properties and Composition

During this experiment, three materials of similar color and category (symmetric, i.e., with identical sides) but different composition were tested. The properties and the nature of the tested materials are presented in Table 1. PhormiTex PHL 20 (PH-20) is an energy-saving gable screen. Luxous-1547 D FR (LD-15) combines good heat-retaining properties with superior light-diffusion and light-transmission qualities. The diffusion brings light to the plants from various directions, reducing the overheating of upper areas. The main function of Luxous-1347 D FR (LD-13) is saving energy through achieving maximum light transmission.

2. Experimental setup

This research was carried out on a building roof in order to get clear sky radiation. A hollow wooden frame was built for the investigation. The bottom part of the frame was covered with black cloth with known radiometric properties (τ_b =0, ρ_b =0.07, ε_b =0.93). The setup had a 3-m^3 volume (3 m width×2 m length×0.5 m height). Fig. 1 demonstrates the dimensions of the setup, positions of the equipment and Laboratory setup. Figs. 2 and 3 depict the radiation exchanged between the sky, screen, and black cloth; the unknown parameters are highlighted in red in the figure. Downward longwave (Q_a and Q_c) and shortwave (S_a and S_c) radiations were measured with a pyrgeometer and pyranometer, respectively, while upward longwave fluxes (Q_b and Q_d) were computed from the difference between the net radiometer and downward fluxes. Upward shortwave radiations (S_b and S_d) were measured using an inverted pyranometer. Two thermocouple wires, with very thin diameters, were used to measure the surface temperature of the thermal screen and black cloth. All measured parameters were recorded at 10-minute intervals and saved in a different data logger. Table 2 shows the list of equipment and data loggers.

3. Measurement of radiative properties during day time

The outgoing shortwave radiation equation above the screen surface (S_b) is given below in $W \cdot m^{-2}$.

$$S_b = \rho_s \cdot S_a + \tau_s \cdot S_d \quad (1)$$

Where ρ_s is the reflectance of screen, τ_s is the transmittance of screen and S_a is the downward sky radiation in $W \cdot m^{-2}$, S_d is the radiations coming from black cloth toward screen in $W \cdot m^{-2}$.

The outgoing shortwave radiation equation over the black surface (S_c) and below the screen surface is given below in $W \cdot m^{-2}$.

$$S_c = \tau_s \cdot S_a + \rho_s \cdot S_d \quad (2)$$

Equations 1 and 2 are used for symmetric materials in order to solve for two unknowns (ρ_s & τ_s). The corresponding

Table 1. Properties of tested materials.

Material \ Properties	Weight ($g \cdot m^{-2}$)	Thickness (mm)	Width of strips (mm)	Energy saving (%)	Composition
PH-20 (Phormium, Belgium)	108	0.27	4	72	100% Polyethylene
LD-13 (Svensson, Korea)	58	0.22	4	47	100% Polyester
LD-15 (Svensson, Korea)	51	0.18	4	47	100% Polyester

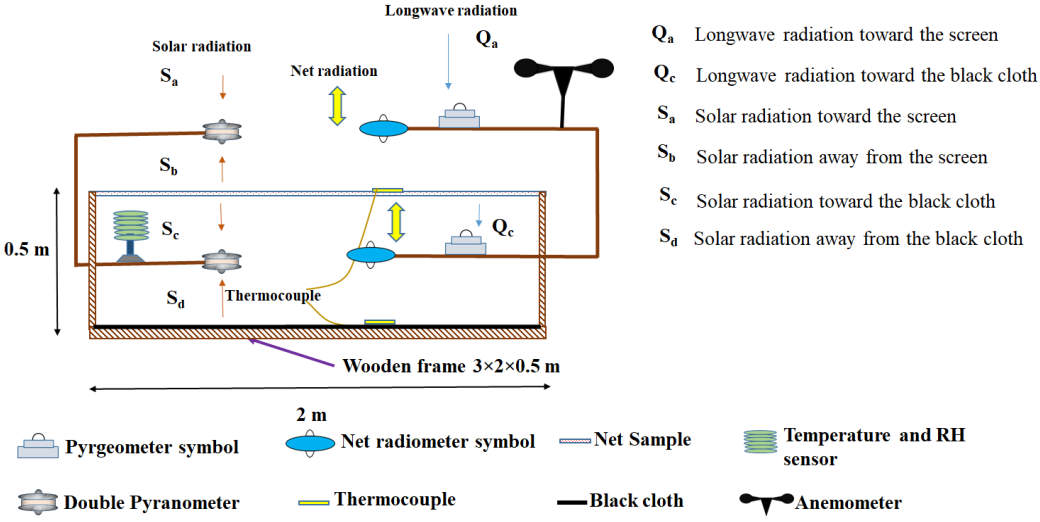

(a)

(b)

Fig. 1. Experimental setup' diagrams (a) Schematic (b) Laboratory arrangement.

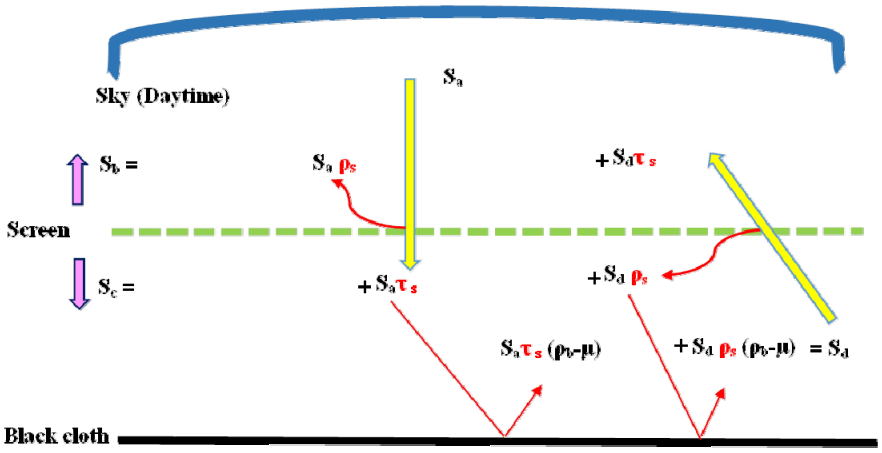

Fig. 2. Ideal drawing of inward (S_a and S_d) and outward (S_b and S_c) radiations from screen.

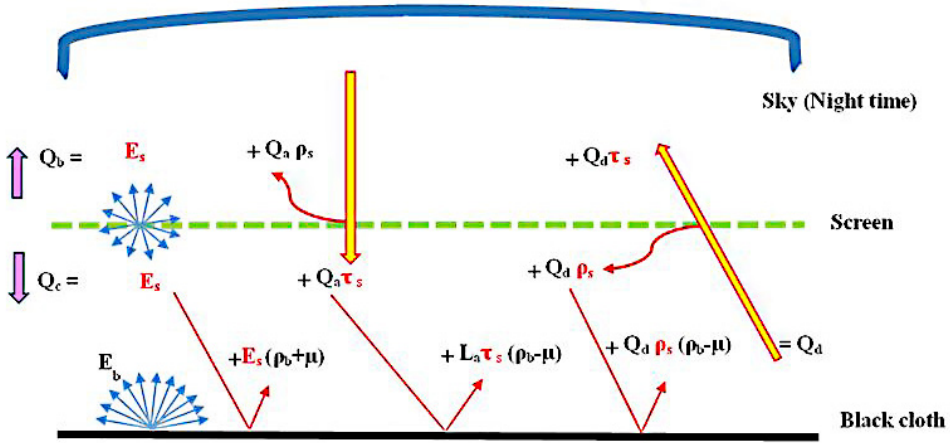

Fig. 3. Ideal drawing of inward (Q_a and Q_d) and outward (Q_b and Q_c) radiations from screen.

Table 2. List of measuring sensors.

Parameter	Unit	Sensor	Range	Data logger
Net longwave radiation	$W \cdot m^{-2}$	NR Lite2 Net Radiometer (Kipp and Zonen, Netherlands)	0.2–100 μm	LR 5041 (Hioki, Japan)
Downward & upward shortwave radiations	$W \cdot m^{-2}$	CMP3 Pyranometer (Kipp and Zonen, Netherlands)	300–2800 nm	LR 5041 (Hioki, Japan)
Downward longwave radiation (Q_a)	$W \cdot m^{-2}$	CGR3 Pyrgeometer (Kipp and Zonen, Netherlands)	4.5–42 μm	21x Micrologger (Campbell Scientific, Inc. USA)
Downward longwave radiation (Q_c)	$W \cdot m^{-2}$	IR02 Pyrgeometer (Hukseflux, Netherlands)	4.5–40 μm	CR300 (Campbell Scientific, Inc. USA)
Temperature/relative humidity	°C / %	Hobo Pro v2 U23-002 (Onset, USA)	-40–70°C 0–100 %	Hobo Pro v2 U23-002 (Onset, USA)
Surface temperature	°C	T-type thermocouple wires	-270–370°C	Hobo UX120-014M (Onset, USA)

absorptance (α_s) is calculated by using Kirchhoff's law of thermal radiation ($\alpha_s = 1 - \rho_s - \tau_s$).

4. Measurement of radiative properties during night time

The outgoing longwave radiation equation above the screen surface (Q_b) is given below in $W \cdot m^{-2}$.

$$Q_b = E + \rho_L \cdot Q_a + \tau_L \cdot Q_d \quad (3)$$

Where E is the emissive power of screen in $W \cdot m^{-2}$, it was determined by Stefan-Boltzmann's law , Q_a is the downward sky radiation in $W \cdot m^{-2}$, Q_d incoming longwave radiation toward the screen, above the black cloth in $W \cdot m^{-2}$, ρ_L is the longwave reflectance of screen, τ_L is the longwave transmittance of screen.

The outgoing long-wave radiation equation over the black surface (Q_c) and below the screen surface is given below in $W \cdot m^{-2}$.

$$Q_c = E + \tau_L \cdot Q_a + \rho_L \cdot Q_d \quad (4)$$

Equation of Q_d is given below

$$Q_d = E_b + (\rho_b + \mu) \cdot E + (\rho_b - \mu) \cdot \rho_L \cdot Q_d + (\rho_b - \mu) \cdot \tau_L \cdot Q_a \quad (5)$$

When equations (3 to 5) were solved simultaneously in Matlab (Matlab R2018B, MathWorks, USA) by iteration method, equation 5 caused compatibility issue even though the number of equations are equal to number of unknowns (E, ρ_L and τ_L). Thus, in order to make these equations

compatible to solve, μ (10^{-6}) is subtracted from reflected portion of $\tau_L \cdot Q_a$ and $\rho_L \cdot Q_d$, and the same number is added into the reflected portion of E in equation 5. Micro (μ) is the smallest assumed number act as tolerance for the reflectance of the black cloth (ρ_b) and with no significant effect on value but it helps to solve these equations. Subtraction and addition is based on the strength of radiation. As emissive power of screen has higher strength than other two factors ($\rho_L \cdot Q_d$ & $\tau_L \cdot Q_a$) because it is coming towards black cloth without striking any surface. E_b is the emissive power of black cloth in $W \cdot m^{-2}$ which was determined by Stefan-Boltzmann's law.

Kirchhoff's law of thermal radiation gives the following equation

$$\tau_L + \rho_L + \alpha_L = 1 \quad (6)$$

Where α_L is the longwave absorptivity.

Measurement of absorption of radiations for 24 hours

The absorbed thermal and solar radiations by the symmetric screen (A) were determined as

$$A = \alpha_L \cdot (Q_a + Q_d) + \alpha_s \cdot (S_a + S_d) \quad (7)$$

Where α_s is absorptivity value in shortwave radiation region.

Over a small interval of time, the energy balance equation, per unit area (m^2), of a horizontal symmetric screen under steady-state natural condition is given by

$$A - 2 \cdot E - 2 \cdot C_{m-a} = 0 \quad (8)$$

Where 'C_{m-a}' is the convective heat transfer from screen to air.

The convective heat transfer coefficient between the symmetric screen and air (h_{m-a}) is given by

$$h_{m-a} = C_{m-a} / (T_m - T_a) \quad (9)$$

Where T_m is the materials surface temperature (K) and T_a surrounding air temperature (K).

The ratio of the buoyancy forces and the inertial forces is expressed as:

$$Gr \cdot Re^{-2} = (g \cdot L \cdot \beta \cdot \Delta T)/v^2 \quad (10)$$

Where g is the gravitational acceleration ($m \cdot s^{-2}$), L is the characteristic length of the screen (m) and we used length of the setup (3 m) as characteristic length, β is the volumetric thermal expansion coefficient (K^{-1}), for an ideal gas β equals inverse of the absolute temperature, ΔT (K) is the temperature difference between screen and surrounding air, and v is the velocity ($m \cdot s^{-1}$).

Results and Discussion

Fig. 4 exhibits the incoming and outgoing shortwave radiations of PH-20. Downward and upward radiations were directly measured by separate pyranometers. Outward radiations S_b and inward radiations S_c were the same in the early morning and later in the evening. The strengths of the radiations, received at the S_c sensor, were weaker due to the low angle of sunlight even though the radiations received at the S_a sensor were greater than two hundred $W \cdot m^{-2}$ from 3:00 pm to 4:00 pm.

Table 3 displays the average values of radiative properties in both the shortwave and longwave regions. Thermal radiations values are adopted from our previous study (Rafiq, 2019). LD-15 and LD-13 showed high values of absorption in the shortwave region. This high absorption can be seen by taking the S_c/S_a, which indicates how much solar radiation passed through the material. Fig. 5 shows that LD-15 and LD-13 showed extremely low values of S_c/S_a as compared to PH-20. Radiations generated by the materials were ignored in this calculation as suggested by previous study (Cohen et al., 2014). The effect of the high absorption can also be seen on the temperature difference graph in Fig. 6. LD-15 and LD-13 had a greater tendency to retain energy, so they exhibited high temperature differences as compared to PH-20, which has a very low absorption value. This table also shows the range of Reynolds numbers over each sample examined. The determination of whether flow is laminar or turbulent is based on the Reynolds number. All the Reynolds numbers calculated for each material were less than 10^5. This shows that the flow over the sample screens was in the laminar range.

The convective heat exchanges between the upper or

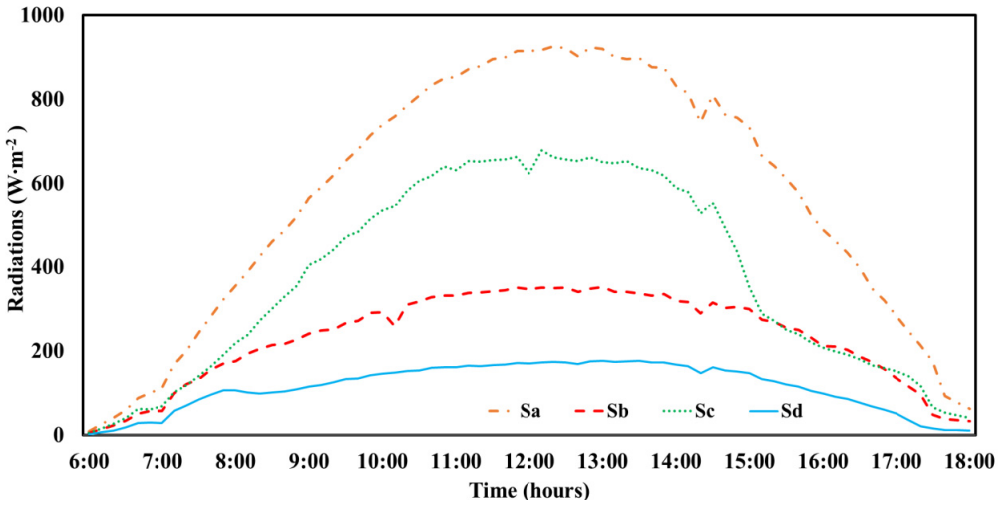

Fig. 4. Inward (S_a and S_d) and outward (S_b and S_c) shortwave radiations for PH-20.

Table 3. Absorption and Reynolds number estimated during experiment.

Sample screen	Absorption		Reynolds number
	shortwave region	longwave region	
PH-20	0.08	0.49	1.77–1.82 E+04
LD-13	0.87	0.46	1.42–1.44 E+04
LD-15	0.89	0.45	8.84–8.92 E+03

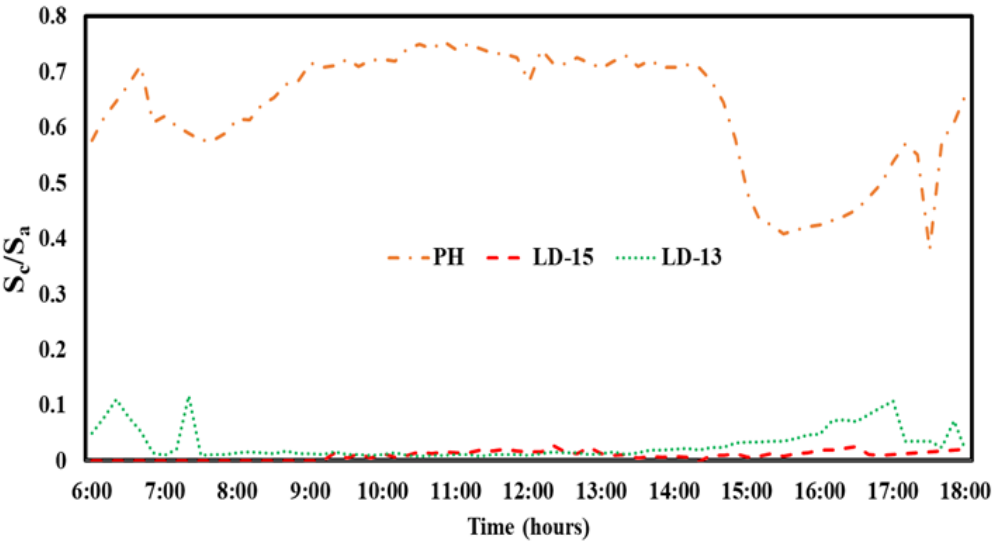

Fig. 5. Ratio between radiations before (S_a) and after (S_c) passing screens.

lower side of the thermal screen and air were calculated, and they are demonstrated in Fig. 7. LD-15 and LD-13 transferred high amounts of heat flux to the air during the daytime because both had high absorption in the shortwave region, which subsequently raised its temperature as compared to ambient air temperature during the daytime. Cloudiness condition can affect the value of heat flux, as the flux is purely based upon solar, sky and materials radiations. So, when one source completely or partially obstructed, it may affect the value. Among these three sources of radiations,

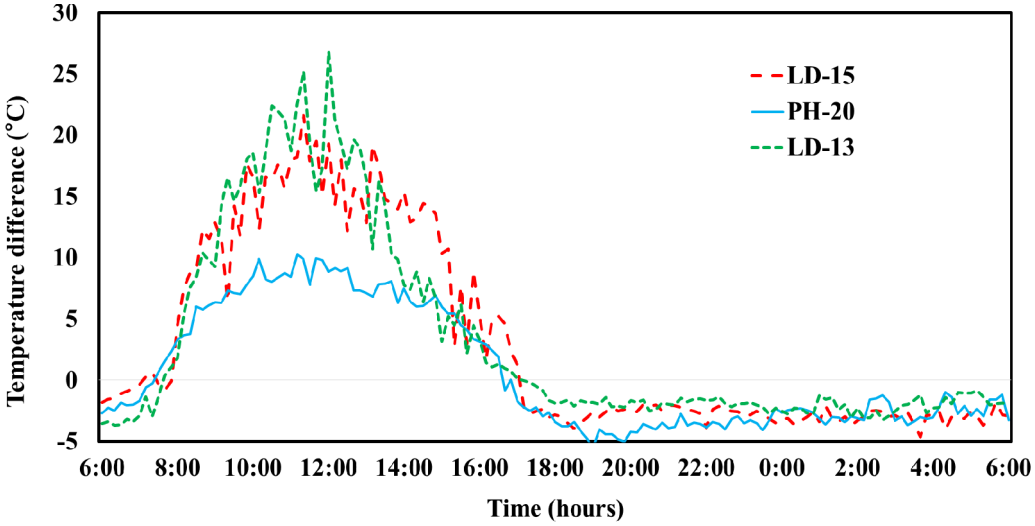

Fig. 6. Difference between ambient and screen temperature calculated for each sample.

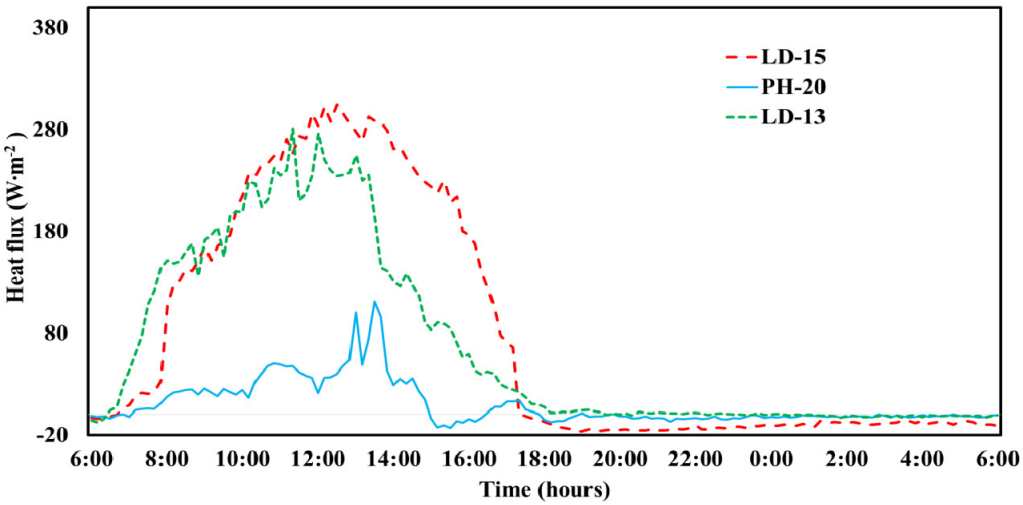

Fig. 7. Time progressions for the convective heat flux.

only the solar radiations can be blocked. LD-15 material showed dome shape curve of heat flux during the daytime which indicate the clear sunny day. Due the presence of partial clouds in the sky, other two materials showed variations in the values.

The time progression of the convective heat transfer coefficients for the thermal screens examined is shown in Fig. 8. Variations in the values are related to the fluctuations in the $Gr \cdot Re^{-2}$ ratio (Abdel-Ghany et al., 2015). Values of heat transfer coefficients mainly depend on the screen–air temperature difference and wind velocity. The amount of convective heat transfer is mainly based upon the local wind velocity, and it has a great effect on the determination of whether the convection is free or forced (Papadakis et al., 1992; Smith, 2010). Thus, wind velocity is required to compute $Gr \cdot Re^{-2}$. Local wind velocity was measured at 1.25 m (from roof surface) height over each sample screen.

During this experiment, it was observed that the value of wind velocity was not more than 1 $m \cdot s^{-1}$. The effect of low wind speed can be seen in Fig. 9. The ratio of $Gr \cdot Re^{-2}$ shows higher values due to the low wind speed, which is directly related to purely free convection. More than 98% of values of this ratio for all tested samples were greater than 1. During the experiment of LD-15 and LD-13, it was observed that the ratio gave higher values during the daytime. The reason of these greater values simply related to the velocity

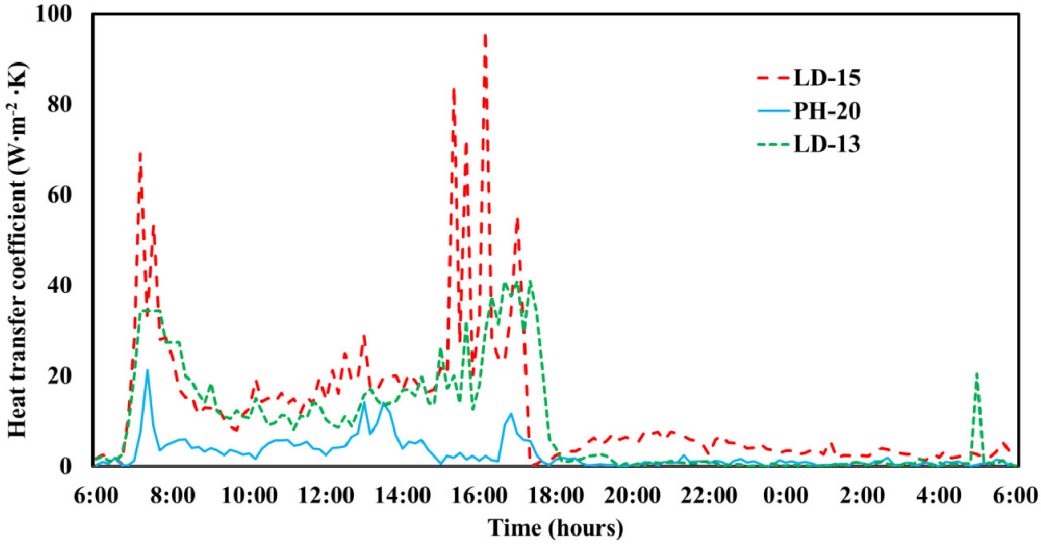

Fig. 8. Time progressions for the convective heat transfer coefficient.

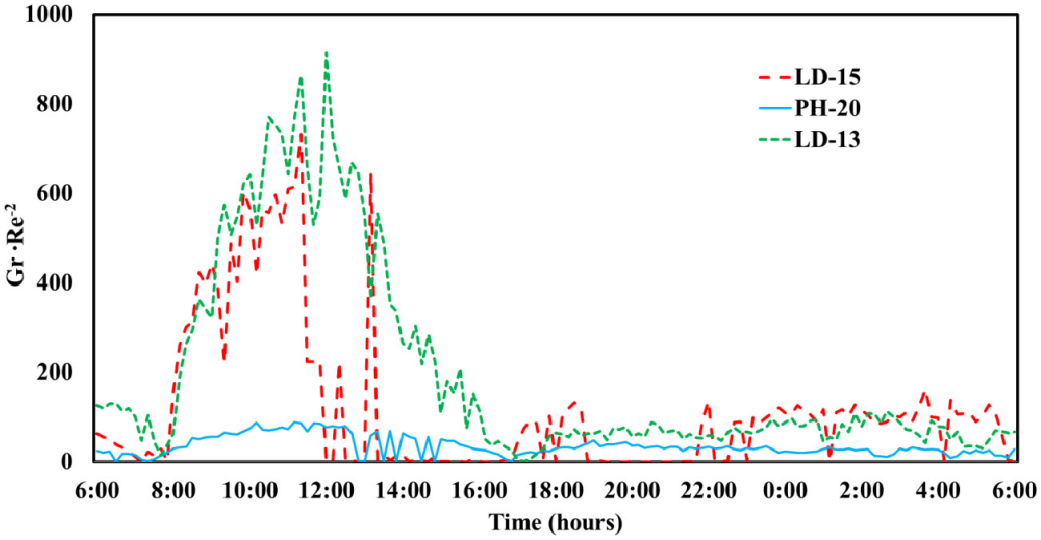

Fig. 9. Time progression for ratio Gr · Re^{-2} to display convection regimes on screen surface.

square factor in the denominator of the equation 10. The other four factors (g, L, β & ΔT) have direct relationship with ratio but have minor effect on the values. Even though temperature difference value increased significantly during the experiment but the impact the on ratio was negligible due the presence of thermal expansion coefficient, as the values of the β were not more than 0.0035. Thus, velocity is the only deciding factor. So, when the value of velocity was less than 1, it was further reduced by the square, and it produced a greater value, which showed the dominant free flow. The wind speed was relatively constant and low, so in this experiment, only the correlation between the temperature difference and convective heat transfer coefficient was drawn. Fig. 10 shows this relation between ΔT and h_{m-a} for LD-15 and LD-13. Equations are also displayed for both materials. These equations can be applied to similar kinds of materials to calculate the convective heat transfer coefficients under similar kinds of environment conditions. Both materials showed that as the temperature difference increases the value of h_{m-a} decreases. In case of LD-15, this decrease was exponential. As it can be seen in the Fig. 10a when temperature difference increased from 0 to 7°C, the value of h_{m-a}

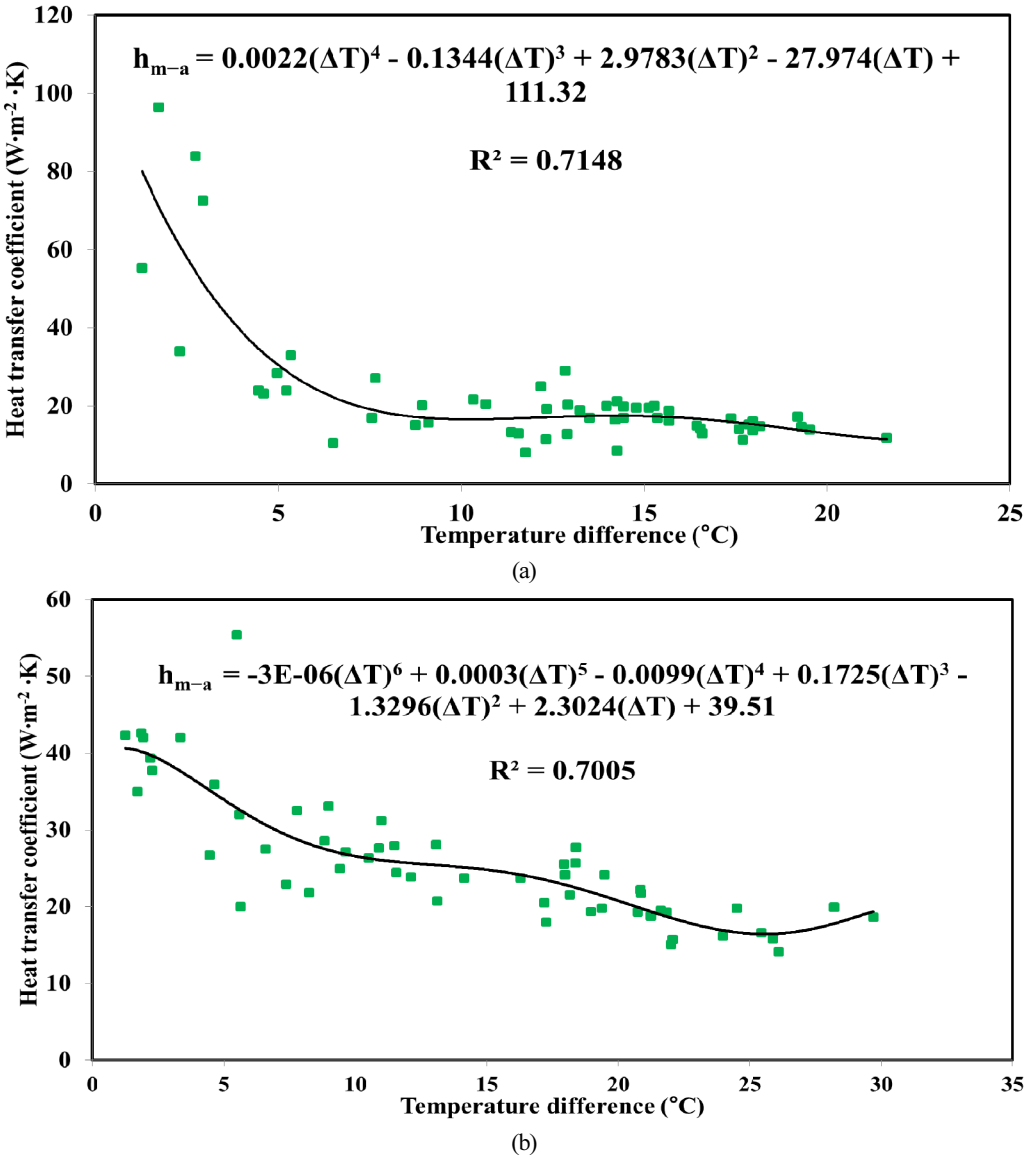

Fig. 10. Relationship between air–screen temperature difference and convective heat transfer coefficient measured during daytime for (a) LD-15 (b) LD-13.

decreased from 88 to 17 W · m^{-2} · K. After this exponential change the value of h_{m-a} remained stable even when the change in temperature difference value reached up to 22°C. In case of LD-13, steady decrease was observed.

Conclusion

A mathematical model was presented to experimentally calculate the convective heat transfer coefficients of energy-saving screens. The procedure was based on radiation balance equations, and it was applied to a wooden frame on which horizontal screens were tacked. Basic parameters required to calculate the coefficient value were radiative properties and air–screen temperature difference. Equipments used for this study were solar and thermal radiation sensors (Net Radiometers, Pyrgeometer, and Pyranometer), temperature sensors (Thermocouple and Hobo Pro v2 U23-002) and anemometer. The convection heat transfer was always purely free for all tested samples, the Reynolds numbers showed that the airflow was in the laminar regime, and the wind velocity in the local area was less than 1 m · s^{-1}. The convective heat transfer coefficients were characterized as

functions of the air–screen temperature difference. It was found that during the daytime, the air–screen temperature difference increased and the screens having high solar radiation absorption (LD-13 and LD-15) indicated a decreasing trend.

Acknowledgements

This research was supported by Basic Science Research Program through the National Research Foundation of Korea (NRF) funded by the Ministry of Education (NRF-2019R1I1A3A01051739). This work was supported by the Korea Institute of Planning and Evaluation for Technology in Food, Agriculture, Forestry and Fisheries (IPET) through Agriculture, Food and Rural Affairs Research Center Support Program, funded by Ministry of Agriculture, Food and Rural Affairs (MAFRA) (717001-7). This research was supported by Kyungpook National University Development Project Research Fund, 2018.

Literature Cited

Abdel-Ghany, A.M., I.M. Al-Helal, M.R. Shady, and A.A. Ibrahim. 2015. Convective heat transfer coefficients between horizontal plastic shading nets and air. Energ. buildings. 93:119-125.

Baïri, A., E. Zarco-Pernia, and J.M.G.D. María. 2014. A review on natural convection in enclosures for engineering applications. The particular case of the parallelogrammic diode cavity. Appl. Therm. Eng. 63(1):304-322.

Cohen, S., M. Möller, M. Pirkner, and J. Tanny. 2014. Measuring radiometric properties of screens used as crop covers. Acta Hortic. 1015:191-200.

Corcione, M., 2008. Natural convection heat transfer above heated horizontal surfaces. 5th WSEAS Int. Conf. on Heat and Mass Transfer (HMT'08), Acapulco, Mexico, January 25-27.

Incropera, F.P., A.S. Lavine, T.L. Bergman, and D. P. DeWitt. 2007. Fundamentals of heat and mass transfer, Wiley.

Issa, S. and W. Lang. 2013. Minimum detectable air velocity by thermal flow sensors. Sensors. 13(8):10944-10953.

Kakac, S., Y. Yener, and A. Pramuanjaroenkij. 2013. Convective heat transfer, CRC press.

Khalifa, A.J.N., 2001. Natural convective heat transfer coefficient–a review:I. Isolated vertical and horizontal surfaces. Energy conversion and management. 42(4):491-504.

Kreith, F., R.M. Manglik, and M.S. Bohn. 2012. Principles of heat transfer, Cengage learning.

Papadakis, G., A. Frangoudakis, and S. Kyritsis. 1992. Mixed, forced and free convection heat transfer at the greenhouse cover. J Agr Eng Res. 51:191-205.

Radziemska, E. and W. M. Lewandowski. 2005. The effect of plate size on the natural convective heat transfer intensity of horizontal surfaces. Heat Transfer Eng. 26(2): 50-53.

Rafiq, A., W.H. Na, A. Rasheed , H.T. Kim, and H.W. Lee 2019. Determination of Thermal Radiation Emissivity and Absorptivity of Thermal Screens for Greenhouse. Protected Hort. Plant Fac. 28(3).

Sharma, K.K. and M. Adelman. 1969. Experimental study of natural convection heat transfer in a non-newtonian fluid: Part II. Horizontal plate. Can. J. Chem. Eng. 47(6):556-558.

Smith, J.O. 2010. Determination of the convective heat transfer coefficients from the surfaces of buildings within urban street canyons. PhD Diss., University of Bath, United Kingdom.

Yang, W.J., H. Takizawa, and D.L. Vrable. 1991. Natural convection from a horizontal heated copper-graphite composite surface. ASME J. Heat Transfer.113(4):1031-1033.

온실 스크린의 대류열전달계수 측정

라피크아딜[1] · 나욱호[2] · 라쉬드아드난[1] · 김현태[3] · 이현우[1,2,4*]

[1]경북대학교 농업토목공학과, [2]경북대학교 농업과학기술연구소, [3]경상대학교 생물산업기계공학과,
[4]경북대학교 스마트농업혁신센터

적 요. 대류열전달은 겨울철 온실 열손실의 중요한 원인이 되며, 일반적으로 복사열에 의한 손실보다 더 크다. 스크린의 대류열전달계수를 자연상태에서 측정한 연구가 수행된 바는 있지만 상하면의 재질이 동일하고 공극이 없는 스크린에 대해서는 적용을 할 수 없는 방법이다. 이러한 재질의 스크린은 한국에서 많이 사용되고 있으나 대류열전달 특성을 파악하는데 많은 어려움이 있는 실정이다. 본 연구에서는 공극이 없는 3가지 종류의 스크린에 대해 대류열전달계수를 구하였으며, 계수를 산정하기 위하여 복사열수지 이론에 근거하여 산정방법을 개발하였다. 실험장치에 스크린을 설치하고 일사량, 장파복사량, 대기온도, 스크린 및 흑색천의 표면온도, 풍속 등을 측정하였다. 스크린의 표면온도와 주변온도의 차이에 따른 대류열전달계수를 산정하였다. 풍속이 거의 없는 상태에서 온도의 차이가 증가함에 따라 계수는 감소하는 것으로 나타났다.

추가 주제어: 대류열전달계수, 스크린, 야간복사계, 흡수율